The Journal of Organic Chemistry

Subscriber access provided by UNIV OF WESTERN ONTARIO

Article

A low temperature crosslinking benzocyclobutene based polymer dielectric for organic thin film transistors on plastic substrates

Rawad Kamal Hallani, Maximilian Moser, Helen Bristow, Maud V. C. Jenart, Hendrik Faber, Marios Neophytou, Emre Yarali, Alexandra F. Paterson, Thomas D. Anthopoulos, and Iain McCulloch

J. Org. Chem., **Just Accepted Manuscript** • DOI: 10.1021/acs.joc.9b02981 • Publication Date (Web): 29 Nov 2019

Downloaded from pubs.acs.org on December 7, 2019

Just Accepted

"Just Accepted" manuscripts have been peer-reviewed and accepted for publication. They are posted online prior to technical editing, formatting for publication and author proofing. The American Chemical Society provides "Just Accepted" as a service to the research community to expedite the dissemination of scientific material as soon as possible after acceptance. "Just Accepted" manuscripts appear in full in PDF format accompanied by an HTML abstract. "Just Accepted" manuscripts have been fully peer reviewed, but should not be considered the official version of record. They are citable by the Digital Object Identifier (DOI®). "Just Accepted" is an optional service offered to authors. Therefore, the "Just Accepted" Web site may not include all articles that will be published in the journal. After a manuscript is technically edited and formatted, it will be removed from the "Just Accepted" Web site and published as an ASAP article. Note that technical editing may introduce minor changes to the manuscript text and/or graphics which could affect content, and all legal disclaimers and ethical guidelines that apply to the journal pertain. ACS cannot be held responsible for errors or consequences arising from the use of information contained in these "Just Accepted" manuscripts.

is published by the American Chemical Society. 1155 Sixteenth Street N.W., Washington, DC 20036

Published by American Chemical Society. Copyright © American Chemical Society. However, no copyright claim is made to original U.S. Government works, or works produced by employees of any Commonwealth realm Crown government in the course of their duties.

A low temperature crosslinking benzocyclobutene based polymer dielectric for organic thin film transistors on plastic substrates

Rawad K. Hallani,[1]* Maximilian Moser,[2] Helen Bristow,[2] Maud V. C. Jenart,[2] Hendrik Faber,[1] Marios Neophytou,[1] Emre Yarali,[1] Alexandra F. Paterson,[1] Thomas D. Anthopoulos,[1] Iain McCulloch[1,2]

Affiliations

[1]King Abdullah University of Science and Technology (KAUST), KAUST Solar Center (KSC), Thuwal 23955-6900, Saudi Arabia

[2]Imperial College London, Department of Chemistry and Centre for Plastic Electronics, London, W12 0BZ, United Kingdom
Rawad.hallani@kaust.edu.sa

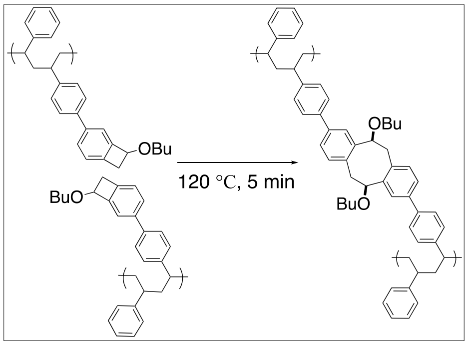

Abstract

The synthesis of a new benzocyclobutene based polymer, **PSBBB**, designed as a dielectric material for use in organic thin film transistors was reported. Compared to conventional benzocyclobutene based materials, the introduction of a butoxide substituent at the 7-position of the benzocyclobutene pendant unit on the polymer allowed **PSBBB** to be crosslinked at temperatures of 120 °C, thus rendering it compatible with the processing requirements of flexible plastic substrates. The crosslinking behavior of **PSBBB** was investigated by Fourier transform-infrared spectroscopy and differential scanning calorimetry, demonstrating crosslinking of the polymer after curing at 120 °C. Bottom-gate bottom-contact organic thin film transistors were fabricated using **PSBBB** as dielectric, affording a comparable performance to other dielectric polymeric materials.

Introduction

High performance organic thin film transistors (OTFTs) are essential components in the fabrication of next generation electronic devices.[1-5] Over the past few decades, significant research effort has been dedicated to improving the performance of OTFTs by optimization of the organic semiconducting materials, with respect to their charge carrier mobilities, ambient stability and compatibility with environmentally friendly and large area, high throughput processing.[6-8]

The use of OTFT semiconductors and dielectrics that are compatible with flexible plastic substrates is particularly desirable, as these can enable new technological applications (*e.g.* flexible displays and electronic skins) and are compatible with roll-to-roll processing techniques, thus contributing to lower manufacturing costs and higher throughput. Although OTFT performance is strongly dependent on the semiconductor used as the active layer,[9-12] the material employed as the dielectric in the transistor architecture can also affect the device operation.[13-15] Dielectric materials should be compatible with solution processing methods, have the versatility to be used in both top and bottom gate transistor devices, provide a trap-free, well defined interface with the semiconductor, possess the required dielectric constant, and be processable at temperatures suitable for use with plastic substrates, such as polyethylene terephthalate (PET), polyethylene naphthalate (PEN), *etc*.[16]

Despite organic semiconductors being typically fabricated with a top-gate bottom-contact (TGBC) OTFT architecture, OTFTs with a bottom-gate bottom-contact (BGBC) structure enable the organic semiconductor acting as channel material to be deposited last, thus facilitating the fabrication and patterning of micron sized electrodes and interconnects prior to application of the semiconductor. In BGBC OTFTs, the dielectric layer is usually a metal oxide (*e.g.* SiO_2, Al_2O_3, *etc.*), however these oxides are often incompatible with flexible plastic substrates due to their brittleness and necessity for high temperature processing.[17, 18] Organic polymer dielectrics (*e.g.* polystyrene, poly(methyl methacrylate), *etc.*) however are compatible with low temperature solution processing techniques, thus making them attractive candidates as dielectric materials. The requirements for top and bottom gate dielectric materials have some significant differences. Top gate dielectrics are required to be deposited on top of the organic semiconductor surface, and therefore the dielectric solvent needs to be completely orthogonal to the semiconductor solubility in order to ensure that it does not dissolve or swell the semiconductor on application, ensuring a clean interface. As a result, solvent choice is restricted to the extremes of polarity, *i.e.* either water based, or more commonly, fluorocarbon based. One example of the latter is the dielectric, CYTOP, a fluoropolymer resin, applied from a fluorosolvent. Although this approach ensures a relatively trap free interface, the subsequent low energy fluoropolymer dielectric surface is difficult to print on top of, which complicates deposition of the gate electrode. Additionally, the low adhesive forces at the fluoropolymer interfaces can facilitate delamination. In the case of bottom gate dielectrics, the solution choice is much wider, as the dielectric/substrate interface does not have such exact electrical requirements, and processed substrates are typically more robust and inert to solvent exposure. On the other hand, the dielectric thin film has to be completely inert to the solution deposition of the organic semiconductor. This requirement has proved extremely difficult to satisfy, particularly as the semiconductor is typically deposited from aggressive solvents that dissolve most common organic dielectric polymers. The obvious way to circumvent this problem is that the dielectric undergoes an *in-situ* crosslinking reaction, thus preventing further dissolution. Common crosslinking chemistries include epoxide ring opening reactions, such as the one used for the SU-8 dielectric, and condensation reactions, such as the one occurring between polyvinylphenol and melamine.[19-23] A key drawback of both of these crosslinking chemistries is that they give rise to products with polar functionalities, which have been demonstrated to function as charge traps at the semiconductor interface, thus also lowering the charge carrier mobility in the semiconductor accumulation layer.[24] Moreover, although high- κ dielectrics are commonly used in the fabrication of OTFT that requires lower turn on voltage, it is found that some organic semiconductors operate better in combination with low-κ dielectrics.[25] This is attributed to the low dipole disorder of the dielectric. Low dipole disorder results in a narrowing of the density of states of the semiconductor at the interface, and as a result, a lower thermal activation is required to activate charge hopping, in comparison to higher dielectric constants, and thus an enhancement in charge carrier mobility is achieved.[14, 25] A solution to this issue is offered by benzocyclobutene (BCB) based resins, a low- κ dielectric, whose crosslinking reaction does not generate any products with polar functionalities.[26] The crosslinking reaction of BCB proceeds by application of thermal energy, which results in the strained cyclobutene moiety to go through an electrocyclic ring opening rearrangement shifting the equilibrium toward the formation of the highly reactive *o*-xylylene intermediate. This intermediate can then undergo a cycloaddition reaction with unsaturated functionalities, such as vinyl units to afford a tetrahydronaphthalene linkage, or with another *o*-xylylene unit, by converting the π-bonds at the termini of the acyclic conjugated π-system to σ bonds, to yield the reactive spirodimer intermediate that can rearrange to the energetically lower 1,2,5,6-dibenzocyclooctadiene linkage.[26, 27]

One key drawback of common BCB dielectrics however, is that their crosslinking reaction necessitates temperatures of over 240 °C, which is unsuitable for flexible OTFTs fabricated on plastic substrates (*e.g.* PET) that typically can only tolerate processing temperatures up to 130 °C.[16, 26] Various research efforts have thus been targeted at foregoing this temperature limitation, whereby the introduction of electron donating alkoxy groups to the cyclobutene ring of the BCB moiety has shown promising results.[28-32] The electrocyclic opening of the alkoxy substituted BCB occurs via a conrotatory process through an outward rotation that leads to a more reactive transition state with comparison to the less preferable inward rotation.[33-35] Consequently, efficient crosslinking can be achieved at lower temperatures.[30-32]

Despite these advances, the application of lower crosslinking temperature BCB dielectrics in electronic devices has to the best of our knowledge not yet been reported in the literature. In this work we thus present the synthesis of a new, low-κ BCB based polymer with a pendant butoxide group on the sp^3 carbon of the cyclobutene functionality, and its subsequent use as polymer dielectric in OTFTs. We employ the indacenodithiophene-benzothiadiazole based polymer, C$_{16}$IDT-BT, as the channel semiconducting polymer in a BGBC device architecture, and demonstrate similar OTFT performances in comparison with state of the art dielectrics.

Results and Discussion

Synthesis of PSBBB. Poly(Styrene-*co*-7-butoxybenzocyclobutene) **(PSBBB)** was prepared as demonstrated in Scheme 1, starting with the iodination of 4-bromophenol, which was synthesized using N-iodosuccinimide to generate **1** in 71% yield.[36] Phenol protection of **1** with HDMS to afford **2** was achieved quantitatively. N-BuLi addition to compound **2** at -78 °C provided compound **3** via an intramolecular rearrangement in 92% yield. Compound **3** was converted to the triflate **4** using triflic anhydride and triethylamine, which was subsequently mixed with cesium fluoride to generate a reactive benzyne intermediate that was cyclized with butyl vinyl ether via a [2+2] cycloaddition reaction to afford compound **5** as an isomeric mixture in 77% yield. The Suzuki coupling of **5** with 4-vinylphenylboronic acid gave compound **6** in 40% yield, which was then polymerized via a free radical polymerization in a 1:1 ratio with a styrene co-monomer using benzoyl peroxide initiator to produce **PSBBB** in 46% yield.

Scheme 1. Synthetic scheme depicting the formation of PSBBB.

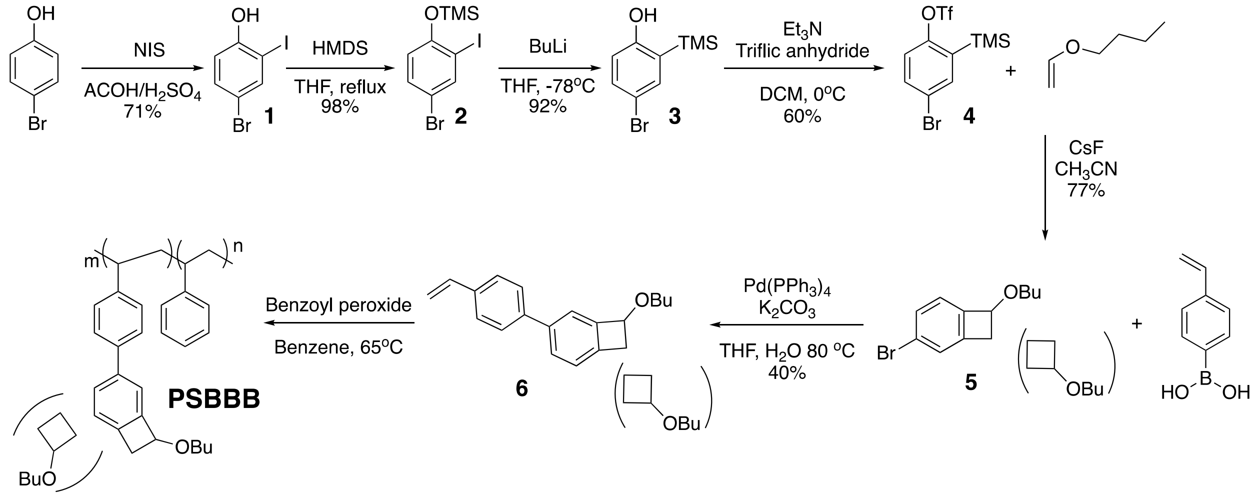

Curing behavior of PSBBB. The crosslinking kinetics of the **PSBBB** polymer developed herein were monitored by a combination of differential scanning calorimetry (DSC), Fourier transform infrared spectroscopy (FTIR) and solvent resistivity measurements.

DSC was employed as a starting analytical technique to evaluate the crosslinking kinetics. The crosslinking of the BCB moiety is an exothermic process due to the release of ring strain from the four-membered ring on the BCB unit.[37] For unsubstituted BCB, this process generally necessitates temperatures >240 °C, as curing onsets around 200 °C with the peak exotherm occurring around 250 °C.[37-39] The inclusion of electron-donating substituents, such as alkoxy groups, on the four-membered ring of the cyclobutene unit has been shown to reduce the curing temperature of BCB analogues.[29, 40] Similar findings were obtained in this study, see Figure 1, as incorporation of a butoxy group on the cyclobutene ring of the BCB unit resulted in an onset of curing at 110 °C, and a peak exotherm at 160 °C for the neat **PSBBB** sample. Consequently, a curing temperature of 120 °C was deemed as appropriate in order to cure **PSBBB** samples.

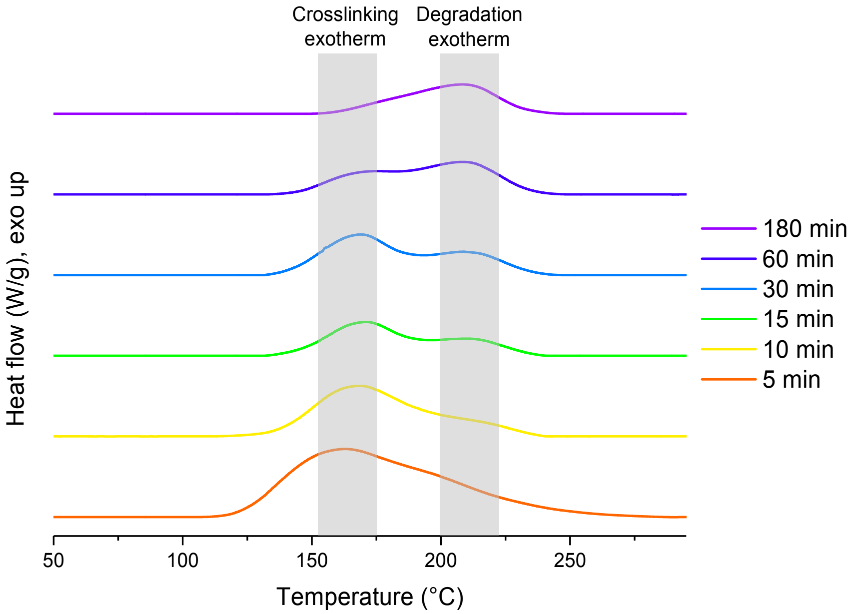

Figure 1. DSC traces obtained for the **PSBBB** samples cured for different time periods at 120 °C and employing a scan rate of 10 K s^{-1}.

As highlighted in Figure 1, curing the samples at 120 °C prior to DSC analysis progressively supressed the exotherm associated with the crosslinking reaction of the BCB unit at 160 °C, with the exotherm being absent after 180 min of curing. During the DSC measurements, a second exotherm at 208°C was noted that progressively became more intense upon increasing the curing time while maintaining a constant temperature of 120 °C. As reported elsewhere,[41] the crosslinked products of the alkoxy substituted BCB based moieties can undergo several reaction pathways, including 1,3-H transfer and transannular bond cleavage, to afford both BCB and alkene containing species.[41] Importantly, while these pathways only occur to a limited extent at 130 °C and 160 °C, the further reaction of the crosslinked products is significantly enhanced at 190 °C. We therefore speculate that the second exotherm recorded for the **PSBBB** samples may be caused by further reaction of the crosslinked products resulting in the formation of several elimination products containing reactive groups, which can then further react in an exothermic crosslinking reaction and generate additional degradation products.[41] The degradation of the samples at elevated temperatures (~200 °C) is also consistent with the results obtained from thermogravimetric analysis (TGA), see Figure S13 in the supporting information, which indicates a change in mass from temperatures around 200 °C. Moreover, curing the **PSBBB** samples at 200 °C, even for short time periods (<5 min), resulted in a colour change from colourless to yellowish-brown and a decrease in film thickness, thus further indicating sample degradation.

The thermal polymerization of **PSBBB** was also monitored with FTIR spectroscopy by annealing the **PSBBB** polymer samples at 120 °C for the same time periods used in DSC. The ring opening process of BCB can be monitored by probing the disappearance of the aromatic ring bending mode of the BCB moiety, which occurs around 1470 cm^{-1}. This process is typically accompanied by the formation of a new vibrational peak that corresponds to the ring bending mode of the newly formed cyclooctadiene. This ring bending mode occurs at a higher wavenumber, typically around 1495 cm^{-1}.[39]

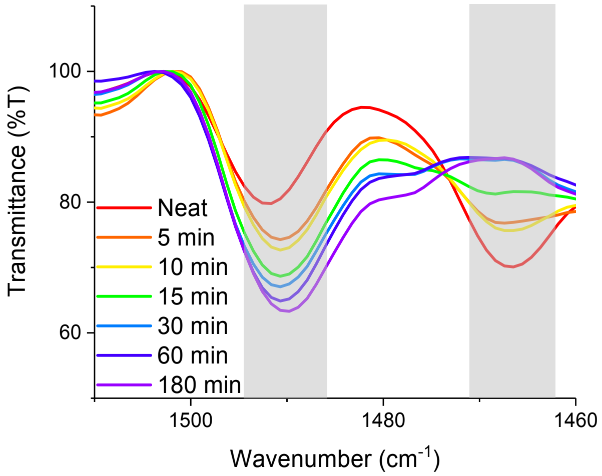

Figure 2. FTIR spectra close-up between 1510 and 1460 cm^{-1} recorded for **PSBBB** samples following curing times between 0-180 min at 120 °C.

The FTIR spectra recorded for **PSBBB** as a function of different curing times at 120 °C in the region of interest between 1510 cm^{-1} and 1460 cm^{-1} are depicted in Figure 2, while the full FTIR spectra can be found in Figure S14 in the supporting information. As demonstrated in Figure 2, the as cast **PSBBB** has characteristic vibrational modes ascribed to the BCB moiety, with a pronounced absorption at 1466 cm^{-1}.[39] Upon increasing the curing time of the sample at 120 °C the peak at 1466 cm^{-1} progressively decreases in intensity, illustrating the consumption of the BCB moiety, while the vibrational feature arising from the cyclooctadiene unit at 1490 cm^{-1} progressively increases in intensity. Together, these changes give rise to an isosbestic point centered around 1475 cm^{-1}, thus indicating the interconversion between the two species.

Evidence of crosslinking of the **PSBBB** samples were also provided by solvent resistivity tests, which demonstrated that already after just 5 min of curing at 120 °C, a crosslinked material was formed that was no longer soluble in a range of organic solvents (toluene, chlorobenzene and dichlorobenzene) that are commonly employed for active layer processing during OTFT fabrication.

Device fabrication. For this study, a C_{16}-IDTBT active layer was employed with gold source and drain electrodes modified with pentafluorothiophenol (PFBT), see Figure 3. Notably, in BGBC transistors the performance of C_{16}-IDTBT has been reported to be significantly worse than in TGBC transistors. In BGBC transistors employing a 300 nm thick polyvinyphenol dielectric C_{16}-IDTBT has previously been shown to exhibit a mobility of ~0.02 $cm^2\ V^{-1}\ s^{-1}$.[42] whereas, in TGBC transistors, much higher mobilities of more than 1 $cm^2\ V^{-1}\ s^{-1}$ are expected. The BGBC transistors fabricated in this work incorporating a 350 nm thick **PSBBB** dielectric layer exhibit a linear regime mobility of

$0.05\ cm^2\ V^{-1}\ s^{-1}$ and a saturation regime mobility of $0.08\ cm^2\ V^{-1}\ s^{-1}$, thus exceeding those of the previously reported BGBC transistors with C_{16}-IDTBT.[42]

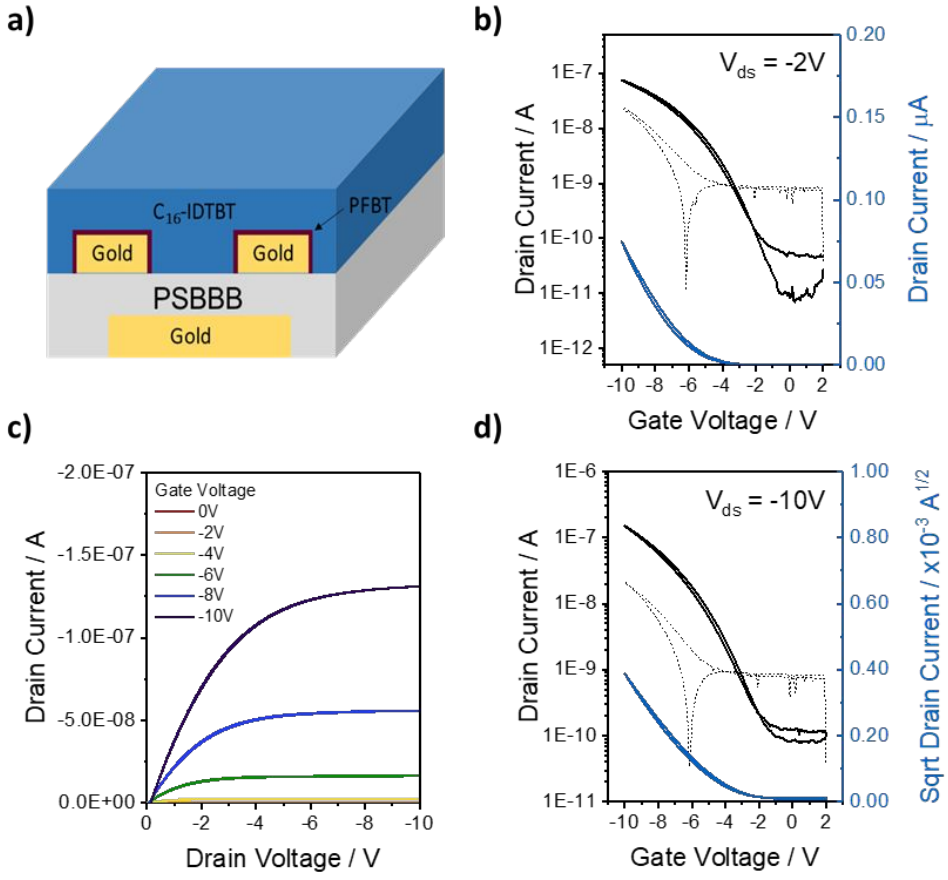

Figure 3. (a) Bottom-gate bottom-contact thin-film transistor architecture of the **PSBBB** based OTFTs. Representative (b) saturation transfer plot, (c) output plot and (d) linear transfer plot for transistors fabricated with each **PSBBB** layer annealed at 120 °C for 5 minutes**.**

Conclusion

In conclusion, the synthesis of a novel benzocyclobutene based dielectric material, **PSBBB,** and its application as a bottom gate dielectric in organic thin film transistors was demonstrated. The incorporation of a butoxide substituent on the benzocyclobutene moiety was shown by DSC and FTIR to enable crosslinking at 120 °C, a temperature significantly lower than for unsubstituted BCB based materials and compatible with the processing conditions incurred by flexible plastic substrates. Notably, curing **PSBBB** for 5 minutes at 120 °C was shown to also incur a good OTFT performance, yielding a saturation mobility of 0.08 cm^2 V^{-1} s^{-1} in C$_{16}$-IDTBT BGBC OTFTs, which exceeds the mobility reported in this transistor architecture with other dielectrics.

Experimental Section

General Procedures. The ^{1}H and ^{13}C NMR spectra were acquired in either a Bruker Avance III 400 MHz NMR spectrometer equipped with a BBFO SmartProbe or a Bruker Avance III 500 MHz NMR spectrometer equipped with a BBFO CryoProbe. Gas chromatography-mass spectrometry (GC-MS) was carried out on an Agilent Technologies 7693. Gel permeation chromatography (GPC) was measured using a PLgel 10 um Mixed-B column on an Agilent Technologies 1260 Infinity system with chlorobenzene as the mobile phase at 80 °C . Fourier transform infrared spectroscopy (FTIR) was conducted on an attenuated total reflectance (ATR) Agilent Cary 630 FTIR spectrometer. Samples for ATR-FTIR measurements were prepared by drop-casting 80 μL of a 20 mg mL^{-1} polymer in toluene solution onto glass substrates and curing the samples on a pre-heated hotplate for either 0 min, 5 min, 10 min, 15 min, 30 min, 60 min or 180 min at 120 °C. The cured polymers were then scraped off the glass substrates and placed on the ATR-FTIR crystal and subsequently analysed. Differential scanning calorimetry (DSC) was performed on a TA Instruments Q20 equipped with a RCS40 refrigerated cooling system. DSC samples were prepared by casting 100 μL of a 20 mg mL^{-1} polymer in toluene solution into weighed DSC pans. Samples were left to dry overnight to ensure complete evaporation of the solvent. The samples were successively sealed with a lid and cured in an analogous fashion as the samples prepared for FTIR measurements. DSC traces of each sample were obtained by heating across a temperature range of 40-300 °C at a heating rate of 10 K min^{-1}. A Bruker Dimension Icon atomic force microscope operating in tapping mode was utilized to characterize the morphology. Micrographs were analyzed with an open source software (Gwyddion).

Thin-film Transistor Fabrication and Characterisation. Bottom gate bottom contact thin film transistors were fabricated on glass substrates cleaned by sequential sonication in acetone and propan-2-ol for 10 minutes each. Onto these one-inch squared glass substrates, gold gate electrodes (45 nm) were deposited by thermal evaporation through a shadow mask. To form the dielectric layer, first **PSBBB** (30 mg mL^{-1} in toluene) was spin coated at 1000 rpm for 45 seconds and annealed for 5 minutes at 120 °C. Next a second layer of **PSBBB** (30 mg mL^{-1} in toluene) was spin-coated at 1000 rpm for 45 seconds and annealed again for 5 minutes at 120 °C. Overall this processing resulted in a 350 nm thick dielectric layer. On top of the dielectric, gold source and drain electrodes (35 nm) were thermally evaporated through a shadow mask. A surface modification was applied by soaking the substrates in pentafluorobenzenethiol (PFBT) (0.005 mol dm^{-3} in propan-2-ol) for 2 minutes before rinsing with propan-2-ol and annealing at 70 °C for 5 minutes. Finally, C$_{16}$-IDTBT (10 mg mL^{-1} in dichlorobenzene) was spin coated at 1200 rpm for 45 seconds and annealed at 100 °C for 5 minutes.Transistors with a channel length of 40 μm and width of 1000 μm were electrically characterised under a N$_2$ atmosphere using a Keysight B2900A Precision Source/Measure Unit.

Dielectric constant calculation of PSBBB. Glass substrates with pre-patterned ITO bottom electrodes were employed to determine the relative permittivity of **PSBBB**. Substrates were initially cleaned by subsequent ultrasonication in de-ionized water, acetone, and 2-propanol for 10 min, respectively. A 10 min UV/O$_3$ treatment was applied directly before the spin coating deposition of **PSBBB** using the same deposition and annealing parameters as for the TFT fabrication. The thermal evaporation of 40 nm Al top electrodes concluded the metal-insulatormetal test structure with a defined area A = 0.1 cm^2. Capacitance-frequency measurements were carried out using a Solartron Si 1260 impedance analyzer, within the frequency range of 100 Hz to 100 kHz, at an AC level of 20 mV and 0 V DC component. The relative permittivity ϵ_r was calculated according to the equation: $\epsilon_r = \frac{C}{A}\frac{t}{\epsilon_0}$, with C = Capacitance, t = thickness, and ϵ_0 = vacuum permittivity. Both, device fabrication as well as measurements, were carried out inside a nitrogen filled glove box. The dielectric constant in Figure S15 was found to be 2.82.

Synthetic Procedures. 4-bromo-2-iodophenol (1). The synthesis of this molecule was achieved following literature procedure.[36] The characterization data are in agreement with the published data.

(4-bromo-2-iodophenoxy)trimethylsilane (2). In a flame dried round bottom flask equipped with a stirring bar **1** (11.4 g, 38.2 mmol, 1.00 eq.) was dissolved in 60 mL of dry THF. To this solution, Hexamethyldisilazane (16 mL, 76 mmol, 2.0 eq) was added dropwise and the resulting reaction mixture was heated in an oil bath to reflux. The reaction was allowed to proceed for 30 min before checking the reaction progress with GC-MS. Once the reaction reached completion, excess solvent was removed under reduced pressure. Due to its poor stability, the crude material was used in the next step without any purification. MS (EI): m/z 372 [M^+]

4-bromo-2-(trimethylsilyl)phenol (3). In a flame dried round bottom flask equipped with a stirring bar, **2** was dissolved (14.8 g, 39.8 mmol, 1.00 eq.) in 200 mL of dry THF. The solution was placed in a dry ice bath, then a 2.5 M *n*-BuLi solution in hexane (17.5 mL, 1.10 eq) was added drop wise and the reaction left stirring at -78 °C for 1 hour. The reaction progress was monitored with GC-MS. The reaction was quenched by addition of a saturated aqueous solution of sodium bicarbonate. The aqueous layer was extracted with DCM and the combined organic layers were dried over magnesium sulfate. Excess solvent was removed under reduced pressure. The crude product was employed in the next step without any further purification. ^{1}H NMR (400 MHz, $CDCl_3$): δ (ppm) 7.42 (d, *J* = 2.5 Hz, 1H), 7.32 – 7.28 (m, 1H), 6.63 (d, *J* = 8.5 Hz, 1H), 0.32 (S, 9H). MS (EI): m/z 246 [M^+]

4-bromo-2-(trimethylsilyl)phenyl trifluoromethanesulfonate (4). In a flame dried round bottom flask equipped with a stirring bar **3** (9.00 g, 36.5 mmol, 1.00 eq.) was dissolved in 80 mL dry DCM, then triethylamine (7.77 mL, 76.8 mmol, 2.10 eq.) was added drop wise. After 15 min the flask was placed in an ice bath before adding triflic anhydride (7.44 mL, 43.9 mmol, 1.20 eq.). The reaction progress was monitored by GC-MS and was deemed complete after stirring for 2 h at 0 °C. The reaction was quenched by addition of water. The aqueous layer was extracted with DCM. The combined organic phases were dried over magnesium sulfate, filtered and concentrated under vacuum. The crude product was purified via silica column chromatography using a 1:1 v/v mixture of PE:DCM to obtain the final product as a colorless oil (8.00 g, 22.0 mmol, 58% yield). ^{1}H NMR (400 MHz, $CDCl_3$): δ (ppm) 7.64 (d, *J* = 2.6 Hz, 1H), 7.57 (dd, *J* = 8.8, 2.6 Hz, 1H), 7.25 (d, *J* = 8.8 Hz, 1H), 0.41 (S, 9H). $^{13}C\{^1H\}$NMR (100 MHz, $CDCl_3$): δ (ppm) 153.7, 138.8, 135.8, 134, 121.6, 121.3, 120.3. HRMS (ESI-TOF) m/z: $[M+H-CH_3]^+$ Calcd for $C_9H_9BrF_3O_3SSi$ 360.9171 Da; Found 360.9177 Da.

3-bromo-7-butoxybenzocyclobutene (5). In a flame dried round bottom flask equipped with a stirring bar cesium fluoride (11.4 g, 75.0 mmol, 6.00 eq.) was added and flask heated to 150°C under high vacuum. After 3 hours, the flask was cooled down and placed under a nitrogen atmosphere. 100 mL of dry acetonitrile were added to generate a slurry to which butyl vinyl ether (4.9 mL, 38 mmol, 3.0 eq.) and **4** (5.70 g, 15.7 mmol, 1.00 eq.) were added dropwise. The mixture was allowed to react at room temperature, after 2 hours the reaction was deemed completed after checking with GC-MS. The reaction was quenched with water and the aqueous phase extracted with DCM. The combined organic layers were dried over magnesium sulfate, filtered and concentrated under reduced pressure. The crude liquid was purified using silica column chromatography employing a 4:1 v/v mixture of PE:DCM as the eluent. Excess solvent was removed under reduced pressure to obtain **5** as a colorless oil (3.01 g, 11.7 mmol, 77% yield). ^{1}H NMR (500 MHz, CDCl$_3$): δ (ppm) 7.50 (d, *J* = 8.8 Hz, 1H), 7.25 (d, *J* = 7.6 Hz, 1H), 6.89 (s, 1H), 5.31 (d, *J* = 10.8 Hz, 1H), 3.72 (m, 1H), 3.66 (m, 1H), 3.53 (m, 1H), 3.2 (m, 1H), 1.7 (m, 2H), 1.48 (m, 2H), 0.99 (t, *J* = 7.4 Hz, 3H). MS (EI): m/z 256 [M$^+$].

3-styrene-7-butoxybenzocyclobutene (6). In a 100 mL round bottom flask equipped with a stirring bar potassium carbonate (3.27 g, 23.5mmol, 3.00 eq) was dissolved in 12 mL of distilled water. The solution was purged with nitrogen for 30 min, before 30 mL of THF were added. **5** (2.0 g, 7.8 mmol, 1.0 eq.) and 4-vinylphenylboronic acid (1.75 g, 11.8 mmol, 1.50 eq.) were then added. The solution was purged for an additional 10 min before Pd(PPh$_3$)$_4$ (270 mg, 0.235 mmol, 0.0300 eq.) was added. The reaction was then heated in an oil bath to 70 °C overnight. The reaction was quenched with water and the aqueous layer extracted with DCM. The organic phases were dried over magnesium sulfate and concentrated under vacuum. The crude product was purified via silica column chromatography using a 95:5 v/v mixture of PE:EA as the eluent. Excess solvent was removed under reduced pressure to obtain the final product as a colourless oil (2.52 g, 9.09 mmol, 77% yield). ^{1}H NMR (500 MHz, CDCl$_3$): δ (ppm) 7.61 – 7.53 (m, 3H), 7.50 (d, *J* = 8.8 Hz, 3H), 7.25 (d, *J* = 7.6 Hz, 1H), 6.79 (dd, *J* = 17.6, 10.9 Hz, 1H), 5.82 (dd, *J* = 17.6, 1.0 Hz, 1H), 5.31 (d, *J* = 10.8 Hz, 1H), 5.12 (dd, *J* = 4.4, 2.0 Hz, 1H), 3.72 (m, 1H), 3.66 (m, 1H), 3.53 (m,1H), 3.2 (m, 1H), 1.7 (m, 2H), 1.48 (m, 2H), 0.99 (t, *J* = 7.4 Hz, 3H). ^{13}C{^{1}H} NMR (125 MHz, CDCl$_3$): δ (ppm) 146.8, 141.7, 141.4, 141.2, 136.4, 128.5, 127.4, 126.6, 123.8, 123, 122.3, 121.5, 113.8, 68.8, 38.4, 32, 19.4, 14.0. HRMS (ESI-TOF) m/z: [M+H]$^+$ Calcd for C20H23O 279.1743 Da; Found 279.1746 Da.

Polymerization method. 2 mL of dry benzene was added to an oven dried microwave vial and purged for 30 min. Styrene (131.1 mg, 1.259 mmol, 1.000 eq.) and **6** (350.0 mg, 1.259 mmol, 1.000 eq.) were added. The resulting solution was purged for 5 min then the reaction was heated in an oil bath to 65°C for 5 min. Benzoyl peroxide (10 mg in 0.1 mL of dry benzene) was then added drop wise and the reaction allowed to run for 16 hours. Excess solvent was removed under reduced pressure and the crude product redissolved in 2 mL of chloroform. The product was precipitated by pouring the chloroform solution into 20 mL of MeOH. The white precipitate was collected by suction filtration and this process was repeated for three additional times. **PSBBB** was obtained as a white powder (220 mg, 46% yield). GPC (Chlorobenzene, 80°C) M_n = 46 kDa, M_w = 91 kDa. ^{1}H NMR (500 MHz, CDCl$_3$): δ (ppm) 7.07 (m, 8H), 6.58(m, 3H), 5.06(s,1H), 3.6 (m, 3H), 3.15 (s, 1H), 1.48 (m, 9H), 0.95 (s, 2H).

Supporting Information

The Supporting Information is available free of charge.

^{1}H and ^{13}C{^{1}H} NMR spectra, GC-MS measurements, TGA traces, FTIR spectra, dielectric constant measurements, AFM data and OFET characterization plots can be found in the supporting information.

Acknowledgments

The research reported in this publication was supported by funding from King Abdullah University of Science and Technology (KAUST).

References

1. Braga, D.; Horowitz, G., High-Performance Organic Field-Effect Transistors. *Advanced Materials* **2009,** *21* (14-15), 1473-1486.
2. Gelinck, G.; Heremans, P.; Nomoto, K.; Anthopoulos, T. D., Organic Transistors in Optical Displays and Microelectronic Applications. *Advanced Materials* **2010,** *22* (34), 3778-3798.
3. Lee, T. H.; Kim, K.; Kim, G.; Park, H. J.; Scullion, D.; Shaw, L.; Kim, M.-G.; Gu, X.; Bae, W.-G.; Santos, E. J. G.; Lee, Z.; Shin, H. S.; Nishi, Y.; Bao, Z., Chemical Vapor-Deposited Hexagonal Boron Nitride as a Scalable Template for High-Performance Organic Field-Effect Transistors. *Chemistry of Materials* **2017,** *29* (5), 2341-2347.
4. Mei, Y.; Diemer, P. J.; Niazi, M. R.; Hallani, R. K.; Jarolimek, K.; Day, C. S.; Risko, C.; Anthony, J. E.; Amassian, A.; Jurchescu, O. D., Crossover from band-like to thermally activated charge transport in organic transistors due to strain-induced traps. *Proceedings of the National Academy of Sciences* **2017,** *114* (33), E6739-E6748.
5. Hallani, R. K.; Thorley, K. J.; Mei, Y.; Parkin, S. R.; Jurchescu, O. D.; Anthony, J. E., Structural and Electronic Properties of Crystalline, Isomerically Pure Anthradithiophene Derivatives. *Advanced Functional Materials* **2016,** *26* (14), 2341-2348.
6. Siegel, A. C.; Phillips, S. T.; Dickey, M. D.; Lu, N.; Suo, Z.; Whitesides, G. M., Foldable Printed Circuit Boards on Paper Substrates. *Advanced Functional Materials* **2010,** *20* (1), 28-35.
7. Zschieschang, U.; Ante, F.; Yamamoto, T.; Takimiya, K.; Kuwabara, H.; Ikeda, M.; Sekitani, T.; Someya, T.; Kern, K.; Klauk, H., Flexible Low-Voltage Organic Transistors and Circuits Based on a High-Mobility Organic Semiconductor with Good Air Stability. *Advanced Materials* **2010,** *22* (9), 982-985.
8. Bettinger, C. J.; Bao, Z., Organic Thin-Film Transistors Fabricated on Resorbable Biomaterial Substrates. *Advanced Materials* **2010,** *22* (5), 651-655.
9. Facchetti, A.; Yoon, M.-H.; Marks, T. J., Gate Dielectrics for Organic Field-Effect Transistors: New Opportunities for Organic Electronics. *Advanced Materials* **2005,** *17* (14), 1705-1725.
10. Wang, Y.; Huang, X.; Li, T.; Li, L.; Guo, X.; Jiang, P., Polymer-Based Gate Dielectrics for Organic Field-Effect Transistors. *Chemistry of Materials* **2019,** *31* (7), 2212-2240.
11. Wang, B.; Huang, W.; Chi, L.; Al-Hashimi, M.; Marks, T. J.; Facchetti, A., High-k Gate Dielectrics for Emerging Flexible and Stretchable Electronics. *Chemical Reviews* **2018,** *118* (11), 5690-5754.
12. Paterson, A. F.; Singh, S.; Fallon, K. J.; Hodsden, T.; Han, Y.; Schroeder, B. C.; Bronstein, H.; Heeney, M.; McCulloch, I.; Anthopoulos, T. D., Recent Progress in High-Mobility Organic Transistors: A Reality Check. *Advanced Materials* **2018,** *30* (36), 1801079.
13. Veres, J.; Ogier, S.; Lloyd, G.; de Leeuw, D., Gate Insulators in Organic Field-Effect Transistors. *Chemistry of Materials* **2004,** *16* (23), 4543-4555.
14. Veres, J.; Ogier, S. D.; Leeming, S. W.; Cupertino, D. C.; Mohialdin Khaffaf, S., Low-k Insulators as the Choice of Dielectrics in Organic Field-Effect Transistors. *Advanced Functional Materials* **2003,** *13* (3), 199-204.

15. Chua, L.-L.; Zaumseil, J.; Chang, J.-F.; Ou, E. C. W.; Ho, P. K. H.; Sirringhaus, H.; Friend, R. H., General observation of n-type field-effect behaviour in organic semiconductors. *Nature* **2005,** *434* (7030), 194-199.

16. Zardetto, V.; Brown, T. M.; Reale, A.; Di Carlo, A., Substrates for flexible electronics: A practical investigation on the electrical, film flexibility, optical, temperature, and solvent resistance properties. *Journal of Polymer Science Part B: Polymer Physics* **2011,** *49* (9), 638-648.

17. Leenen, M. A. M.; Arning, V.; Thiem, H.; Steiger, J.; Anselmann, R., Printable electronics: flexibility for the future. *physica status solidi (a)* **2009,** *206* (4), 588-597.

18. Sekitani, T.; Zschieschang, U.; Klauk, H.; Someya, T., Flexible organic transistors and circuits with extreme bending stability. *Nature Materials* **2010,** *9* (12), 1015-1022.

19. Teh, W. H.; Dürig, U.; Drechsler, U.; Smith, C. G.; Güntherodt, H.-J., Effect of low numerical-aperture femtosecond two-photon absorption on (SU-8) resist for ultrahigh-aspect-ratio microstereolithography. *Journal of Applied Physics* **2005,** *97* (5), 054907.

20. Vicca, P.; Steudel, S.; Smout, S.; Raats, A.; Genoe, J.; Heremans, P., A low-temperature-cross-linked poly(4-vinylphenol) gate-dielectric for organic thin film transistors. *Thin Solid Films* **2010,** *519* (1), 391-393.

21. Tozlu, C.; Mutlu, A., Poly(melamine-co-formaldehyde) methylated effect on the interface states of metal/polymer/p-Si Schottky barrier diode. *Synthetic Metals* **2016,** *211*, 99-106.

22. Matters, M.; de Leeuw, D. M.; Vissenberg, M. J. C. M.; Hart, C. M.; Herwig, P. T.; Geuns, T.; Mutsaers, C. M. J.; Drury, C. J., Organic field-effect transistors and all-polymer integrated circuits. *Optical Materials* **1999,** *12* (2), 189-197.

23. Drury, C. J.; Mutsaers, C. M. J.; Hart, C. M.; Matters, M.; Leeuw, D. M. d., Low-cost all-polymer integrated circuits. *Applied Physics Letters* **1998,** *73* (1), 108-110.

24. Conradie, E. H.; Moore, D. F., SU-8 thick photoresist processing as a functional material for MEMS applications. *Journal of Micromechanics and Microengineering* **2002,** *12* (4), 368-374.

25. Veres, J.; Ogier, S.; Leeming, S.; Cupertino, D.; Khaffaf, S. M.; Lloyd, G., *Gate insulators influencing electronic transport in organic FETs*. SPIE: 2003; Vol. 5217.

26. Burdeaux, D.; Townsend, P.; Carr, J.; Garrou, P., Benzocyclobutene (BCB) dielectrics for the fabrication of high density, thin film multichip modules. *Journal of Electronic Materials* **1990,** *19* (12), 1357-1366.

27. Marks, M. J.; Erskine, J. S.; McCrery, D. A., Products and Mechanism of the Thermal Crosslinking of Benzocyclobutene-Terminated Bisphenol A Polycarbonates. *Macromolecules* **1994,** *27* (15), 4114-4126.

28. Oppolzer, W., Intramolecular Cycloaddition Reactions of ortho-Quinodimethanes in Organic Synthesis. *Synthesis* **1978,** *1978* (11), 793-802.

29. Chino, K.; Takata, T.; Endo, T., Polymerization of o-quinodimethanes, 1. Radical polymerization of 1-methoxy-o-quinodimethane formed in situ by thermal isomerization of 1-methoxy-benzocyclobutene. *Macromolecular Rapid Communications* **1996,** *17* (5), 339-345.

30. Hayes, C. O.; Chen, P.-h.; Thedford, R. P.; Ellison, C. J.; Dong, G.; Willson, C. G., Effect of Ring Functionalization on the Reaction Temperature of Benzocyclobutene Thermoset Polymers. *Macromolecules* **2016,** *49* (10), 3706-3715.

31. Dobish, J. N.; Hamilton, S. K.; Harth, E., Synthesis of low-temperature benzocyclobutene cross-linker and utilization. *Polymer Chemistry* **2012,** *3* (4), 857-860.

32. Pugh, C.; Baker, J. S.; Storms, W. K., Synthesis of a Polymerizable Benzocyclobutene that Undergoes Ring-Opening Isomerization at Reduced Temperature. *Synlett* **2014,** *25* (01), 148-152.

33. Houk, K. N.; Spellmeyer, D. C.; Jefford, C. W.; Rimbault, C. G.; Wang, Y.; Miller, R. D., Electronic control of the stereoselectivities of electrocyclic reactions of cyclobutenes against incredible steric odds. *The Journal of Organic Chemistry* **1988,** *53* (9), 2125-2127.

34. Jefford, C. W.; Bernardinelli, G.; Wang, Y.; Spellmeyer, D. C.; Buda, A.; Houk, K. N., Torquoselectivity in the electrocyclic conversion of benzocyclobutenes to o-xylylenes. *Journal of the American Chemical Society* **1992,** *114* (4), 1157-1165.

35. Keisuke, C.; Takeshi, E., Prediction of Thermal Isomerization Temperatures of Substituted Benzocyclobutenes to o-Quinodimethanes by Semi-Empirical Molecular Orbital Calculation. *Letters in Organic Chemistry* **2011,** *8* (2), 138-142.

36. Desroches, M.; Morin, J.-F., Synthesis and properties of a trapezoid shaped macrocycle with different [n]yne units. *RSC Advances* **2017,** *7* (28), 17117-17121.

37. Kirchhoff, R. A.; Bruza, K. J., Benzocyclobutenes in polymer synthesis. *Progress in Polymer Science* **1993,** *18* (1), 85-185.

38. Tong, J.; Diao, S.; Jin, K.; Yuan, C.; Wang, J.; Sun, J.; Fang, Q., Benzocyclobutene-functionalized poly(m-phenylene): A novel polymer with low dielectric constant and high thermostability. *Polymer* **2014,** *55* (16), 3628-3633.

39. Stokich, T. M.; Lee, W. M.; Peters, R. A., Real-Time FT-IR Studies Of The Reaction Kinetics For The Polymerization Of Divinyl Siloxane Bis-Benzocyclobutene Monomers. *MRS Proceedings* **1991,** *227*, 103.

40. Chino, K.; Takata, T.; Endo, T., Polymerization of o-Quinodimethanes Bearing Electron-Donating Groups in Situ Formed by Thermal Isomerization of Benzocyclobutenes. *Macromolecules* **1997,** *30* (22), 6715-6720.

41. Gies, A. P.; Spencer, L.; Rau, N. J.; Boopalachandran, P.; Rickard, M. A.; Kearns, K. L.; McDougal, N. T., Thermally Induced Cross-Linking and Degradation Reactions of Benzocyclobutene-Based Polymers. *Macromolecules* **2017,** *50* (6), 2304-2319.

42. Zhang, X.; Bronstein, H.; Kronemeijer, A. J.; Smith, J.; Kim, Y.; Kline, R. J.; Richter, L. J.; Anthopoulos, T. D.; Sirringhaus, H.; Song, K.; Heeney, M.; Zhang, W.; McCulloch, I.; DeLongchamp, D. M., Molecular origin of high field-effect mobility in an indacenodithiophene–benzothiadiazole copolymer. *Nature Communications* **2013,** *4* (1), 2238.